The role of implantation-induced point defects for the redistribution of oxygen in silicon at high-temperature processing

R. Kögler,[a] X. Ou, W. Skorupa, and W. Möller
Forschungszentrum Dresden-Rossendorf, PF 510119, D-01314 Dresden, Germany

(Received 25 June 2008; accepted 26 September 2008; published online 17 November 2008)

The excess of implantation-induced point defects controls the oxygen redistribution in silicon during a high-temperature treatment, such as in separation-by-implanted-oxygen, and defines the energy-dose window for the formation of a perfect homogeneous and planar buried oxide layer. Quantitative relations are given between the distribution of the initially generated excess defects and the finally formed oxide layer. Implantation-induced defects also explain the depth positions of different oxide precipitate layers and of silicon islands inside the oxide layer. Other defects as, e.g., dislocations, which form during thermal treatment, may relocate the energy-dose window toward a lower oxygen dose. © *2008 American Institute of Physics*. [DOI: 10.1063/1.3020530]

I. INTRODUCTION

Separation-by-implanted-oxygen, commonly known as the SIMOX process,[1] is the original manufacturing technique for the fabrication of silicon-on-insulator (SOI) material. It consists of the high-dose O implantation at temperatures $T \geq 500$ °C and a long-term annealing at temperatures $T \geq 1350$ °C. The technology was developed during the 1990s to industrial maturity. More recently, the scientific interest in SIMOX decreased as other promising production techniques for SOI material were invented. However, the SIMOX process is not entirely theoretically understood yet and is ongoing with perfection. The main problem is the very high O ion dose necessary to finally achieve a homogeneous planar buried oxide (BOX) layer. A high ion dose is not only an economic disadvantage, but it also results in a high level of implantation defects. The state-of-the-art technology employs defect engineering in order to reduce the O dose, e.g., the modified low dose (MLD) implantation[2,3] and the internal oxidation (ITOX).[4–7] The redistribution of implanted oxygen during high-temperature annealing, as in SIMOX, proceeds by coarsening or Ostwald ripening.[8,9] This process is characterized by the oxygen migration directed against the total concentration gradient via the dissolution of small oxide precipitates and the growth of big ones. Ostwald ripening of oxide precipitates in silicon was theoretically well explained by computer simulations.[8,10,11] However, there is a gap in the understanding of the final stage of the BOX formation that also includes precipitate coalescence and phase separation. Recently, we reported that implantation-induced defects control the BOX formation.[12] The present paper shows in more detail that the consideration of radiation defects generated by oxygen implantation can explain a couple of characteristics observed in SIMOX processing for a wide range of oxygen doses. A simple model is applied for the radiation defects taking into account only excess defects. Such defects remain in silicon after the complete local recombination of irradiation-generated vacancies and interstitials.[13–15] The depth distributions of excess vacancies (V_{ex}) and excess interstitials (I_{ex}) were calculated by simulations using the computer code transport and range of ions in matter.[16,17]

II. EXCESS DEFECTS AND THE ENERGY-DOSE WINDOW

The so-called energy-dose (ED) window is the experimental finding that a planar homogeneous BOX layer can only be formed as the O ion energy fits with the O dose.[18–22] A satisfactory explanation by theory is still missing. When the oxygen dose for a given ion energy is below the ED window the oxide layer is not continuous and consists of isolated oxide precipitates. For a dose above the ED window a continuous but inhomogeneous oxide layer is formed including silicon islands. Calculations of the V_{ex} and I_{ex} profiles[17] revealed that for implants in accordance with the ED window the relation $x_J = x_B$ is fulfilled, where x_J is the position at which the vacancy region abruptly changes to the interstitial region and x_B is the upper (near-surface) interface of the BOX. Moreover, the oxygen concentration in the BOX region after implantation is found to be always above a well-defined value, $c_C = c_O(x_J) = 1.9 \times 10^{22}$ cm^{-3}.[12] This situation is demonstrated in Fig. 1 for one example of an ED window implant. The thickness of the BOX [Fig. 1(a)] formed after the complete redistribution of the implanted oxygen is closely related to the O dose $d_B = \Phi_O / c_{ox}$, where c_{ox} is the O concentration in SiO_2. There is also a close relation between the final BOX [formed after thermal treatment, Fig. 1(a)] and the distribution of implantation defects [in the as-implanted state, Fig. 1(b)]. Apparently, this relation is important for the complete redistribution of oxygen in order to form a narrow planar homogeneous BOX layer.

The effect of implantation defects can be explained by the different influences of vacancies and interstitials on the growth rate of oxide precipitates because the SiO_2 formation in silicon is accompanied by a significant volume expansion. Vacancies assist oxide precipitation, whereas it is restrained by the presence of interstitials. At the junction between the excess vacancy region and the excess interstitial region x_J, the precipitate growth rate strongly decreases. Such a de-

[a]Electronic mail: r.koegler@fzd.de.

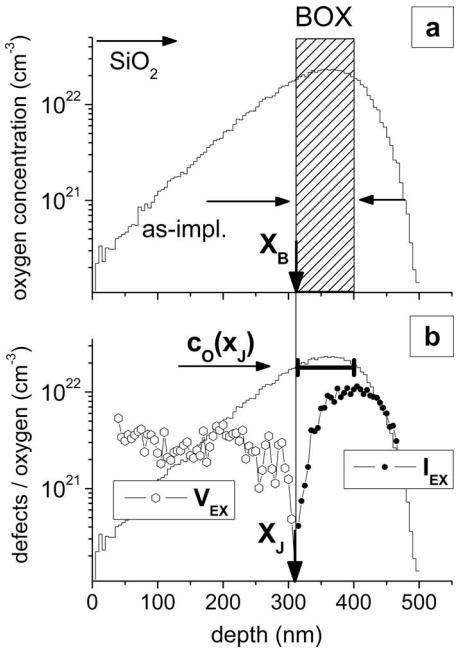

FIG. 1. (a) The calculated depth distribution for O implanted into Si with 150 keV to 4.1×10^{17} cm^{-2} (inside the ED window) and the corresponding BOX (hatched area) are shown. The position x_B indicates the Si/SiO_2 interface. Arrows demonstrate the direction of O redistribution. (b) For comparison the excess vacancy profile (V_{ex}) and the excess interstitial profile (I_{ex}) are shown below. The position x_J marks the change from the vacancy region to the interstitial region. The horizontal bar indicates the BOX position centered at the maximum O concentration.

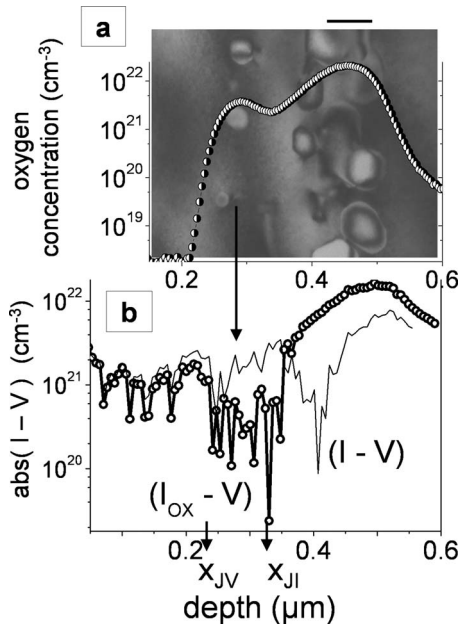

FIG. 2. (a) Overlay of the XTEM image and the oxygen profile measured by SIMS (taken from Ref. 24) for implantation of 200 keV, 3×10^{17} O cm^{-2} at 550 °C into Si and annealing at 1250 °C for 5 h in Ar. The bar above the XTEM image indicates the thickness of the corresponding BOX. (b) The calculated local difference in interstitials (I) and vacancies (V) is shown below. Implantation-generated excess defects (I-V) are presented by a thin line, whereas the thick line with circles (I_{ox}-V) also takes into account interstitials generated by the oxide formation. The boundaries x_{JV} and x_{JI} of the junction region are indicated.

crease in the precipitate growth rate acts like a barrier for the progression of oxygen redistribution (by Ostwald ripening) and results in an accumulation of oxygen at depth positions close to x_J. The accumulation of oxygen results in an undesired growth of precipitates. A precipitate grown to a size comparable with the thickness of the BOX cannot be redissolved.[23] Therefore, the parity $x_J=x_B$ is the "best choice" for a complete redistribution of oxygen and to realize a narrow BOX. The O concentration of $c_C=1.9\times10^{22}$ cm^{-3} [Fig. 1(b)] defines a "critical" concentration. Above this threshold ($c_O\geq c_C$) oxide formation in the BOX predominantly proceeds by coalescence[12] and the region is rather characterized by silicon precipitates located in an oxide substrate.

Figure 2(a) shows an overlay of a cross section transmission electron microscopy (XTEM) image and the oxygen depth distribution measured by secondary ion mass spectrometry (SIMS) for O implantation with 200 keV to a dose of 3×10^{17} cm^{-2} after annealing.[24] The dual layer structure of the oxide precipitates is typical and was often reported in the literature for similar experimental conditions.[25–28] In Fig. 2(a) the O dose is below the ED window (4.1×10^{17} cm^{-2}) and the maximum O concentration after implantation was 1.55×10^{22} cm^{-3}, slightly lower than the threshold c_C. Therefore, the oxide precipitates do not coalesce to a continuous oxide layer, even for a stronger thermal treatment. The precipitates in the upper layer at $x\approx0.25$ μm are stable as they are relatively large sized compared to the corresponding BOX thickness indicated by the bar. In Fig. 2(b) the difference in the radiation-induced interstitials and vacancies is presented by the (I-V) curve as calculated for the implant in Fig. 2(a). Even though the absolute value of I-V is given, the regions of V_{ex} and I_{ex} are well distinguishable by the pronounced minimum at $x_J=0.4$ μm. Additional (oxidation-induced) interstitials are generated taking into account the reaction of implanted oxygen with the silicon substrate. The volume expansion by the factor of 2.27 due to the reaction $2O+Si\rightarrow SiO_2$ increases the amount of interstitials to $I_{ox}=I+0.626O$, where I denotes the irradiation-generated interstitials and O the implanted oxygen. In this way the local ratio of excess vacancies and excess interstitials is changed. Hence, the curve (I_{ox}-V) represents the modified distribution of excess defects including both radiation-induced and oxidation-induced interstitials. In that case the total amount of excess interstitials is increased and the I_{ex} region is enlarged to $x=0.33$ μm. There is a region $x_{JV}\leq x\leq x_{JI}$ in Fig. 2(b) without a clear dominance of one type of point defects, which represents a junction region instead of an abrupt junction. The boundaries at interstitial side and vacancy side are denoted x_{JI} and x_{JV}, respectively. Thus the V_{ex} region is constricted to the range from the surface to the depth of 0.24 μm. The surface-near oxide precipitate layer [Fig. 2(a)] is formed just at the position of the junction region [Fig. 2(b)]. This agreement supports the idea of oxygen accumulation in the region where the oxide precipitate growth rate falls. The implication of interstitial ejection during oxidation may be a high local strain around the growing precipitates. However, the whole layer structure relaxes during the high temperature annealing by dissolution of the small precipitates and surface swelling.

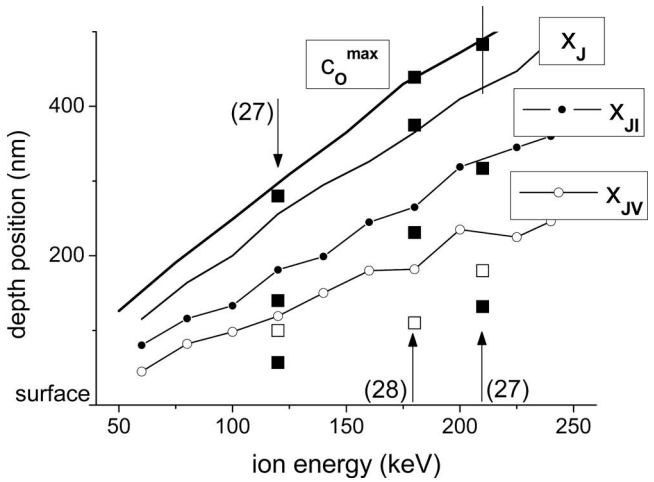

FIG. 3. Calculated depth positions of the maximum concentration c_O^{max} and of the junction depth x_J are shown for oxygen implantation as a function of ion energy. The junction region according to Fig. 2(b) is the spacing between the boundaries x_{JI} (dots) and x_{JV} (circles). For comparison positions of experimentally observed oxide precipitate layers (squares) are included. Hollow squares represent weak (first dissolved) precipitate layers. Experimental results were taken from Ono and Ogura (Ref. 27) and Tamura *et al.*(Ref. 28).

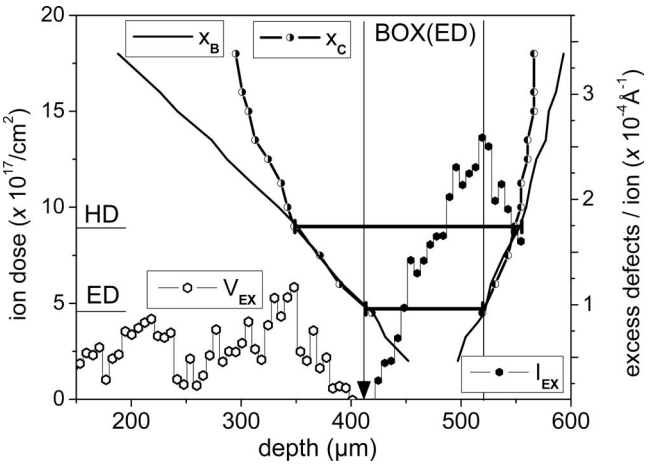

FIG. 4. Calculated depth profiles of excess vacancies (V_{ex}) and excess interstitials (I_{ex}) for Si implanted with 200 keV O ions (right scale). The arrow at x=410 nm indicates the position of the junction (x_J) between V_{ex} and I_{ex}. The depth positions of the BOX interfaces (x_B) and of the critical O concentration (x_C) are shown vs the O dose (left scale). Two horizontal bars demonstrate the extension of the BOX for O implantation in the ED window and for stoichiometric O implantation at the HD threshold $c_O^{max}=c_{ox}$.

III. DENOTATION OF OXIDE PRECIPITATE LAYERS

The denotation of different oxide layers or precipitate layers in the literature is confusing. For a dual structure [as in Fig. 2(a)] the main layer is conventionally denoted as the R_P layer and the overlying layer the D_P layer. This wording is based on the argument that there are two depth positions of preferential oxide precipitate growth: these are positions of the maximum oxygen concentration $x(c_O^{max})$ and of the maximum damage concentration D_P (the maximum density of nucleation sites).[18] However, the calculated R_P position (the mean projected ion range) for O implantation is about 10% above the position of c_O^{max} due to the asymmetry of the profile. Moreover, the maximum damage position D_P is only 5% below the junction $D_P \approx 0.95 x_J$. Therefore, R_P and D_P may easily be mixed up with $x(c_O^{max})$ and x_J. The frequently used term $1/2R_P$ characterizes the excess vacancy cluster formation (and impurity gettering) somewhere between the surface and x_J. It does not describe an exact depth position because the as-implanted excess vacancy distribution is mostly a "flat" function [e.g., V_{ex} in Fig. 1(b)], and there is no definitely predictable trigger point for the vacancy clustering.

IV. ACCUMULATION OF OXIDE PRECIPITATES IN LAYERS

Figure 3 shows the calculated depth positions for preferential oxygen accumulation at $x(c_O^{max})$ and x_J (replacing the terms R_P and D_P). In addition the boundaries of the junction region are indicated, as calculated for oxidation-induced interstitial generation [see Fig. 2(b)]. Experimentally observed positions of oxide precipitate layers are also shown in Fig. 3.[27,28] There are four positions of preferred precipitate growth: $x(c_O^{max})$, x_J, the junction region between x_{JV} and x_{JI}, and eventually the V_{ex} region. In the V_{ex} region the precipitate growth is assisted by the free volume, whereas in the junction region and at x_J oxygen is accumulated due to the local decrease in the precipitate growth rate. However, the observation of all these precipitate layers strongly depends on the experimental conditions, especially on the thermal treatment. Generally, the dissolution of the oxygen precipitates begins at the surface, where oxygen out diffusion may play a role[27] and proceeds toward the maximum concentration of oxygen. The most stable (fastest growing) precipitates for conventional SIMOX processing are those at the maximum oxygen concentration, which finally form the BOX. It should be noted that also multilayer structures were reported for O doses well above the high dose (HD) threshold for which the oxygen concentration exceeds the stoichiometry, $c_O^{max} \geq c_{ox}$.[18,28,29] Such structures can be explained in terms of alternating vacancy-type and interstitial-type layers, which were experimentally proven for Ge-implanted silicon.[30]

V. AS-IMPLANTED POINT DEFECTS AND THE FINAL BOX POSITION

Computer simulations successfully explain the formation of separate precipitate layers during redistribution of oxygen for low dose ion implantation.[8,10,11] The point defect distribution furthermore explains the origin of the ED window and some characteristics of the continuous oxide layer formation after high dose implantation, as the distribution of silicon islands inside the BOX. In Fig. 4 the position and the thickness of the BOX as functions of dose are compared with excess defect profiles. The BOX interfaces are shown by the x_B lines (as demonstrated in Fig. 1) and the depth position x_C means the depth for which the oxygen concentration reaches the critical concentration $c_O(x_C)=c_C$. The distributions V_{ex} and I_{ex} in Fig. 4 are unchanged in their depth position as the O dose increases, whereas the BOX is extended (mainly toward the surface). For O doses in the range between ED and HD the coalescence region ($c_O \geq c_C$) fits with the BOX region $x_C=x_B$. Another general characteristic of O implantation can also be seen in Fig. 4, the bottom SiO_2/Si BOX interface is closely located at the region of maximum interstitial con-

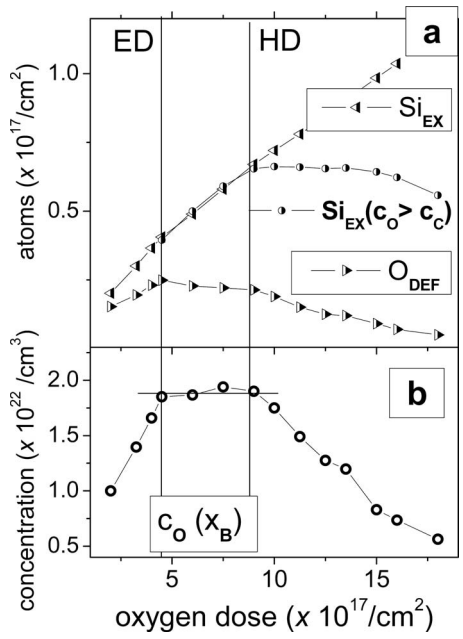

FIG. 5. (a) The calculated amount of silicon excess (Si_{ex}) and of oxygen deficit (O_{def}) in the BOX region is shown for implantation of 200 keV O ions in dependence of the ion dose. In addition, the amount of silicon excess is indicated in the coalescence dominated region [$Si_{ex}(c_O \geq c_C)$] where the oxygen concentration is above the critical concentration c_C. (b) The ED window and the HD threshold $c_O^{max}=c_{ox}$ are marked. The as-implanted oxygen concentration at the surface-near BOX interface $c_O(x_B)$ is shown vs dose.

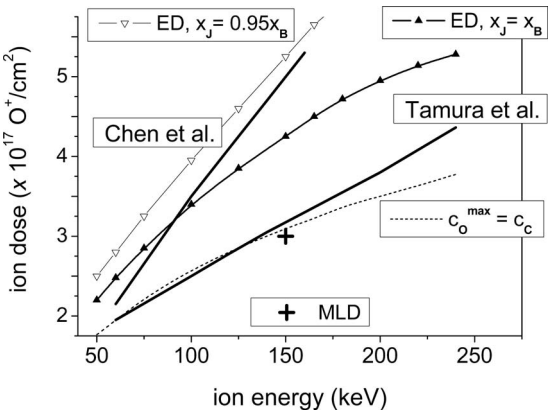

FIG. 6. Comparison of two data sets of ED windows (fat curves) experimentally determined by Chen *et al.* (Ref. 19) and by Tamura *et al.* (Ref. 28). The calculated ED window region spans between the ED curves for a BOX position at $x_J=x_B$ (full triangles) and at $x_J=0.95x_B \approx D_P$ (hollow triangles). The O dose, for which the maximum concentration of oxygen is the critical concentration $c_O^{max}=c_C$, is given by the dashed line. Curves were slightly smoothed. The cross shows the result for MLD implantation as reported by Holland *et al.*(Ref. 2).

centration. Silicon inclusions in the BOX preferentially remain in this region with the highest interstitial concentration, where the oxide precipitate growth is suppressed. In fact, for higher O doses silicon islands were observed in the most cases in this region close to the bottom BOX interface.[18,19,26,29,31]

VI. REDISTRIBUTION OF OXYGEN AND SILICON

In Fig. 5(a) the fractions of oxygen and silicon in the BOX are shown in the as-implanted state. The amount of oxygen in the profile tails, outside the BOX, is identical to the deficit of oxygen inside the BOX (O_{def}). Furthermore, the silicon atoms inside the BOX region, which are not needed to form SiO_2, are silicon excess atoms (Si_{ex}). Both oxygen deficit atoms and silicon excess atoms are redistributed during thermal treatment into and out of the BOX, respectively. As demonstrated in Fig. 5(a), the amount of silicon excess is much higher than the oxygen deficit. Considering the low mobility of Si atoms in SiO_2 the redistribution of the silicon excess out of the BOX constitutes a more serious problem that increases with the increasing O dose. Thus it appears that the conditions for the formation of a perfect SOI structure are deteriorated as the O dose is enhanced above the ED window. In Fig. 5(b) the as-implanted oxygen concentration at the BOX interface x_B is given. In the dose range between ED and HD the concentration is at its maximum value $c_O^{max}(x_B)=c_C$. This result corresponds to the relation $x_C=x_B$ in Fig. 4. In the dose range above the HD threshold both the deficit of oxygen in the BOX and the oxygen concentration at the BOX interfaces decrease. Hence, the oxygen redistribution mainly proceeds inside the BOX region already during ion implantation due to the high mobility of O in SiO_2.[18]

VII. INFLUENCE OF OTHER DEFECTS

There is accordance in the literature about the ED window; however, the different experimental data sets of the ED window significantly deviate from each other. Some of those experimental results show perfectly formed SOI structures for O doses well below the calculated ED window.[18,21,22,25] In Fig. 6 ED window data from two research groups are reported, which investigated the BOX formation more systematically. For low ion energy both ED windows are close together, but there is a considerable divergence of the trend with increasing ion energy. The calculated ED curve for $x_J=x_B$ overestimates the O dose for ion energies below 75 keV due to the point defect recombination at the near surface.[12] For ion energies above 75 keV the ED curve for $x_J=x_B$ is between both experimental curves. However, the statistical uncertainty of the Monte Carlo simulations results in an area of validity between the ED curves calculated for $x_J=0.95x_B$ and $x_J=x_B$.[12] Note that the position $x_J=0.95x_B$ approximately agrees with the damage maximum D_P. Only the experimental data of Chen *et al.*[19] fall into this region, whereas the data of Tamura *et al.*[22] are close to the curve calculated for O doses for which the maximum oxygen concentration just reaches the critical concentration for precipitate coalescence c_C. These differences may be explained considering other defects beside the implantation-induced excess defects. Such defects are oxidation-induced interstitials [Fig. 2(b)] and extended structural defects, such as amorphous regions or dislocations, the latter are formed during the thermal treatment. Such defects are heterogeneous nucleation sites for oxygen precipitates. The mobility of oxygen along dislocations may be enhanced as the coalescence of oxide precipitates connected by dislocations is enforced.[2,32] In-plane dislocations inside the BOX region and dislocations connecting the precipitates in the junction region with those in the BOX are

crucial for the oxygen accumulation in only one single layer.[26,28] These defects are "good" ones in contrast to threading dislocations penetrating the whole top-Si layer.[22] MLD is based on the controlled introduction of an amorphous region and of dislocations.[32] Holland *et al.*[2] reported the formation of a continuous BOX layer by MLD implantation with 150 keV ions to 3×10^{17} O cm^{-2}. These parameters are in agreement with the ED window data of Tamura *et al.*[22] (Fig. 5). Hence, the formation of a perfect BOX layer for O doses below the calculated ED window is attributed to other defects, e.g., dislocations.

VIII. DEFECT ENGINEERING

Defect engineering in SIMOX processing may proceed or not by relatively small changes in the process parameters. For instance, an increase in the oxygen fraction in the annealing atmosphere may result in the in diffusion of atmospheric oxygen into the silicon substrate. Atmospheric oxygen can contribute to the growth of a BOX layer (ITOX effect).[4] However, it depends on the subtleties of the annealing, as the temperature ramping rate or the presence of a surface capping layer, whether the atmospheric oxygen contributes to BOX formation or the implanted oxygen contributes to the growth of the surface oxide layer (negative ITOX effect).[27,31,33] The scattering of the experimental data may be explained in this way. It is worth to note that oxidation-induced interstitials generated by surface oxidation are also introduced into the top-Si layer. Those interstitials emitted by the moving SiO_2/Si interface may contribute to dissolve oxide precipitates and assist oxygen redistribution. Ogura[34] reported on the high quality of a BOX interface formed directly in front of the surface oxide interface. This result can be understood by the combined effect of the introduced oxygen atoms and interstitials. At last, the BOX formation is also influenced by the crystal orientation dependent oxidation rate of precipitates. It results in differing ED data for SIMOX in Si(100) and Si(111) substrates.[21]

IX. SUMMARY

The experimentally well established ED window in SIMOX processing is caused by the distribution of the implantation-induced excess of point defects. It is determined by two relations: $x_J=x_B$ and $c_O(x_J=x_B)=c_C$. Suitable conditions for the formation of a planar homogeneous BOX layer exist if the BOX interfaces are in agreement with x_J (upper interface) and with the maximum of I_{ex} (deeper interface). The oxygen dose according to the ED window is defined by the position and thickness of a BOX corresponding to the relations given above, if extended structural defects and ITOX are absent. Implantation-induced defects can also explain the positions of oxide precipitate layers formed in ion implanted silicon during high-temperature treatment and of silicon islands remaining inside the BOX close to the bottom interface. Other defects modify the ED window. Such defects are oxidation-induced interstitials and extended structural defects, e.g., dislocations formed during the thermal treatment. Structural defects connecting oxide precipitates enforce their coalescence and may relocate the ED window at a lower oxygen dose. Therefore, smart defect engineering is a promising tool in order to further reduce the O dose in SIMOX processing.

[1] See *SIMOX*, edited by M. J. Anc (The Institution of Electrical Engineers, Stevenage Herts, 2004).
[2] O. W. Holland, D. Fathy, and D. K. Sadana, Appl. Phys. Lett. **69**, 674 (1996).
[3] D. K. Sadana and J. P. de Souza, Defect induced buried oxide (DIBOX) for throughput SOI, patent application: US 5,930,643 A (27 July 1999) and US 259,137 B1 (10 July 2001).
[4] Y. Takahashi, T. Ishiyama, and M. Tabe, Appl. Phys. Lett. **65**, 2987 (1994).
[5] U. Gösele, E. Schroer, and J.-Y. Huh, Appl. Phys. Lett. **67**, 241 (1995).
[6] S. Nakashima, T. Katayama, Y. Miyamura, A. Matsuzaki, M. Kataoka, D. Ebi, M. Imai, K. Izumi, and N. Ohwada, J. Electrochem. Soc. **143**, 244 (1996).
[7] A. Matsumura, I. Hamaguchi, K. Kawamura, T. Sasaki, S. Takayama, and Y. Nagatake, Microelectron. Eng. **66**, 400 (2003).
[8] S. Reiss and K.-H. Heinig, Nucl. Instrum. Methods Phys. Res. B **84**, 229 (1994).
[9] K.-H. Heinig, B. Schmidt, M. Strobel, and H. Bernas, Mater. Res. Soc. Symp. Proc. **650**, R9.6.1/O14.6.1 (2001).
[10] S. Reiss and K.-H. Heinig, Nucl. Instrum. Methods Phys. Res. B **112**, 223 (1996).
[11] S. Strobel, S. Reiss, K.-H. Heinig, and W. Möller, Radiat. Eff. Defects Solids **141**, 99 (1997).
[12] R. Kögler, X. Ou, W. Skorupa, and W. Möller, Appl. Phys. Lett. **92**, 181906 (2008).
[13] O. W. Holland, L. Xie, C. Nielson, and D. S. Zhou, J. Electron. Mater. **25**, 99 (1996).
[14] A. Brown, O. Kononchuk, G. A. Rozgonyi, S. Koveshinikov, A. P. Knights, P. J. Simpson, and F. Gonzalez, J. Appl. Phys. **84**, 2459 (1998).
[15] V. C. Venezia, D. J. Eaglesham, T. E. Haynes, A. Agarwal, D. C. Jacobson, H.-J. Gossmann, and F. H. Baumann, Appl. Phys. Lett. **73**, 2980 (1998).
[16] J. Biersack and L. G. Haggmark, Nucl. Instrum. Methods **174**, 257 (1980).
[17] R. Kögler, A. Peeva, J. Kaschny, W. Skorupa, and H. Hutter, Nucl. Instrum. Methods Phys. Res. B **186**, 298 (2002).
[18] S. Nakashima and K. Izumi, J. Mater. Res. **8**, 523 (1993).
[19] M. Chen, J. Chen, W. Zheng, L. Li, H. C. Mu, Z. X. Lin, Y. H. Yu, X. Wang, and G. Y. Wang, J. Vac. Sci. Technol. B **19**, 337 (2001).
[20] M. Chen, X. Wang, J. Chen, Y. Dong, X. Liu, Y. Yu, and X. Wang, Appl. Phys. Lett. **80**, 880 (2002).
[21] H. Iikawa, M. Nakao, and K. Izumi, J. Mater. Res. **19**, 3607 (2004).
[22] M. Tamura, K. Tokiguchi, H. Seiki, M. Ishimaru, and H. Mori, Appl. Phys. A: Mater. Sci. Process. **81**, 1375 (2005).
[23] S. Mantl, Mater. Sci. Rep. **8**, 1 (1992).
[24] R. Kögler, A. Mücklich, L. Vines, D. Krecar, A. Kuznetsov, and W. Skorupa, Nucl. Instrum. Methods Phys. Res. B **257**, 161 (2007).
[25] A. Ogura, J. Electrochem. Soc. **145**, 1735 (1998).
[26] S. Bagchi, S. J. Krause, and P. Roitman, Appl. Phys. Lett. **71**, 2136 (1997).
[27] H. Ono and A. Ogura, J. Appl. Phys. **87**, 7782 (2000).
[28] M. Tamura, M. Ishimaru, K. Hinode, K. Tokiguchi, H. Seki, and H. Mori, Jpn. J. Appl. Phys., Part 1 **45**, 7592 (2006).
[29] Y. Tan, B. Johnson, S. Seraphin, J. Jiao, M. J. Anc, and L. P. Allen, J. Mater. Sci. Mater. Electron. **12**, 537 (2001).
[30] R. Kögler, A. Peeva, A. Mücklich, F. Eichhorn, and W. Skorupa, Appl. Phys. Lett. **88**, 101918 (2006).
[31] B. Johnson, Y. Tan, P. Anserson, S. Seraphin, and M. J. Anc, J. Electrochem. Soc. **148**, G63 (2001).
[32] J. B. de Souza, C. A. Cima, P. F. P. Fichtner, and H. Boudinov, J. Appl. Phys. **95**, 877 (2004).
[33] K. Kawamura and T. Motooka, J. Electrochem. Soc. **153**, G1078 (2006).
[34] A. Ogura, Appl. Phys. Lett. **74**, 2188 (1999).